Contents lists available at ScienceDirect

Wear

journal homepage: http://www.elsevier.com/locate/wear

Abrasive wear behaviour of 27MnB5 steel used in agricultural tines

Ádám Kalácska [a,*], Patrick De Baets [a], Dieter Fauconnier [a], Florian Schramm [b], Ludger Frerichs [b], Jacob Sukumaran [a]

[a] Ghent University, Department of Electrical Energy, Systems & Automation, Soete Laboratory Technologiepark 46, B-9052, Zwijnaarde, Ghent, Belgium
[b] Technische Universität Braunschweig, Institute of Mobile Machines and Commercial Vehicles, Langer Kamp 19a, D-38016, Braunschweig, Germany

ARTICLE INFO

Keywords:
Steel
Agricultural tine
Three-body abrasion
Micro-scale abrasion
Degree of penetration
DEM soil flow

ABSTRACT

Understanding the wear mechanisms in wear parts is a crucial element of tribological investigation, particularly in agricultural applications where the knowledge about abrasive micro-mechanisms of soil engaging tools are limited. In the current research, symmetrical skew wedge cultivator tines of 27MnB5 steel were wear tested to investigate the change in mass, linear dimensions, hardness and microstructure, aiming at prolonging the lifetime of these parts through design and material. The wear mechanisms were identified and characterized by non-contact 3D optical profilometry. Test results clearly shows a zone specific wear micro-mechanism based on the tine geometry. The cutting edge of the tine can be segmented into micro-cutting and micro-ploughing zone. Vickers hardness and microstructural analysis were performed on the cross-section of the sliding interface. Tribo-layer was observed on the worn surface. Degree of penetration from the wear scratches was calculated to justify the wear micro-mechanisms. A Discrete Element Method (DEM) model was developed to investigate the soil flow during the tillage process. The model results and field test wear scars are in good agreement with each other with respect to the wear patterns.

1. Introduction

In agricultural machinery wear parts are often made of specific steels, e.g. tillage tools, which are strongly subjected to abrasive wear are produced from 27MnB5 [1]. Tillage is defined as the preparation of the soil by mechanical agitation [2]. In the farming process, before planting or seeding a crop, the soil needs to be in a good state. The processes of soil preparation are executed by specially designed agricultural tools. These tools are divided into two categories according to their functionality, which are cutting (primary tillage) and shaping (secondary tillage) of the soil [2]. Soil cutting tools can be further classified according to their shape as being similar to a straight wedge (shares of potato harvesters), a skew wedge (ploughshares, L-hoe blades) or a symmetrical skew wedge (A-hoe blades and double blades, shares of planters and ridgers, subsoilers) [3]. Most research has been focused on determining wear resistance and analysis of wear distribution of skew wedge shape ploughshares [3]. In this investigation symmetrical skew wedge tine is analysed.

Abrasive wear of tillage tools is a major problem for farmers all over the world. The hard mineral particles of different soils can cause severe wear and damage in working machine elements [4], in this research primary cutting tools are investigated. In 1986, the National Research Council of Canada made an estimation of the total cost originating from the wear in the agricultural sector is around $ 940 million per year [5]. The tines which experience severe wear during operation do not only result into increase in fuel and energy consumption but overall low work quality with the risk of tool loss and thus danger of subsequent processes. Replacement of tines costs not only money but also time, which is critical in the season of seeding and planting crops [6,7]. From the economic perspective it is clear that research on the wear behaviour of agricultural tools is critical. To increase the wear resistance, the wear process has to be completely understood. Several wear investigations on tillage tools were already performed, however those reports do not focus on the wear mechanisms [3,8–10].

Tillage wear is commonly classified as open three-body low-stress abrasive wear [11]. Abrasive wear is defined as material removal due to sliding contact with abrasive particles or a rough surface [12], where in three-body wear the particles are loose and may move relatively to each other or rotate while sliding across the material, while in open three-body abrasion the surfaces are far apart and do not influence the wear of each other [13]. The wear of tillage tools is classified as open three-body low stress abrasion, because there is a small compression

* Corresponding author.
E-mail address: adam.kalacska@ugent.be (Á. Kalácska).

https://doi.org/10.1016/j.wear.2019.203107
Received 29 March 2019; Received in revised form 12 September 2019; Accepted 26 October 2019

load on the particles, which slide and impact on only one wearing surface [14]. Often a dry contact condition is experienced in tillage processes, very high moisture content is to be avoided because it influences the traction. Wear response is based on the properties of the contacting bodies. The second body, which is the abrasive/sand (quartz) particle, plays a significant role in controlling the wear properties of the process itself [7].

The most common method to investigate wear rate and compare different materials is based on measurement of the weight loss of the material after a stipulated sliding distance [3,8,9]. Ferguson et al. [7] measured the mass loss in dry and stony conditions and found a constant mass loss rate over the lifetime of the shares without a running-in phase. Additionally, geometrical dimension is widely used to extract wear data. Natsis et al. [8] used the average cutting edge thickness to investigate the wear on a mouldboard ploughshare. Owsiak [3] measured the thickness of the tine at different locations along the cutting edge. It was evident from his analysis that the wear rate decreased with increasing distance and some running-in behaviour was present. The cutting edge of the tine close to the tine tip experienced severe wear. This was explained with the stress concentration which is largest around the tine tip. Owsiak [3] defined three important dimensions next to the thickness measurements, which are tip length, width and edge length. It was found that the losses were not constant, the tip length decreased at a higher pace during the initial sliding and stabilized only after reaching 30% of the total lifetime. It was also observed that part of the cutting edge close to the share point was subjected to the largest wear, while the wear of the edge decreased as the distance from the share point increased. It was explained with the stress concentration in the soil around this zone, after blunting of the tip the impact was distributed over a large zone [3]. This may indicate the presence of different micro-mechanisms on different tine segments. The wear process that affects tillage tools is categorized as open three-body low stress abrasion, composed out of four micro-mechanisms: micro-cutting, micro-ploughing, micro-fatigue and micro-cracking [15].

The wear measurement techniques in previous investigations [3, 8–10] are often based on mass loss or dimensional changes and the wear micro-mechanisms of the wear process are not characterized. The type of wear mechanism influences the wear rate [16] so understanding the wear micro-mechanisms is necessary for tribological characterization. An important parameter that can give information about the dominant wear mechanism on a surface is the degree of penetration (D_p) of the wear scratch. It is calculated by dividing the depth of the wear scratch with the half width as defined by Hokkirigawa et al. [17]. The D_p partly illustrates the severity of wear and the micro-mechanism by itself it can act as an indicator to decide the operational regime between mild and severe wear. Low D_p values indicates micro-ploughing with plastic deformation of the material while higher D_p values (>0.3) indicates micro-cutting phenomena with continuous chip formation and wear of the material. Within a single tine different wear modes can be present, the different state of stress is exerted on the different segments of the tine. This also influences the flow of the abrasive particles in contact with the tine during the ploughing and the compaction of the soil. In this investigation the flow of abrasive particles is analysed with DEM and compared to the results obtained from the field test.

The Discrete Element Method (DEM) is characterized by the free interaction of individual solids with each other and was originally developed by Cundall and Strack for investigations in rock mechanics [18]. The simulation method has been widely used in various disciplines, especially in recent years. In agricultural engineering, the DEM is used to simulate field products such as potatoes or maize, but also for soil cultivation. For this purpose, very different aspects are investigated. The most frequent investigations concern the parameterisation of the soil and the resulting forces and loads on the tools to be investigated. Relative particle-geometry displacements were used by Coetzee and Els to predict the position and shape of the shear lines in front of the geometry in the form of a horizontally aligned plate [19]. Soil mixing is an essential task of soil tillage; the mixing effects were investigated by process and tool parameters with the DEM. Barr investigates the effect of narrow point openers on the basis of the parameters of the furrow profile such as the loosened area, ridge height, immersion area, furrow backfilling and lateral soil insertion [20]. The tool shape was used by Shmulevich with the DEM to optimize soil tillage tools. It was based on four designs, which were evaluated with regard to the forces occurring but also on the basis of the mixing performance [21]. In addition to the effect of a single tool in the soil, Hang investigated the influence of the lateral distance between two tools for optimal soil mixing [22]. Zhang analysed adjustments of the geometry for a better working pattern in soil tillage with regard to better clod crushing [23]. The subject of wear in agricultural soil tillage has so far only been examined to a limited extent. The work of Graff and Tong should be mentioned here as an example. Graff focuses fundamentally on the modelling of wear in the DEM. The model is validated using a cylindrical solid as a reference that has been moved through the soil [24]. Tong investigates the effect of a change in the surface morphology on the wear behaviour of a Farrer's scallop [25]. A study of particle movement with the DEM along critical areas, such as the cutting edge of the tine, was not carried out to the authors' knowledge.

Due to the detrimental effects of tillage tool wear (replacement cost, timing, energy) investigations have already been performed on the determination of the wear influencing factors. These factors are material properties (hardness, toughness and microstructure), soil type (particle hardness, size, angularity and compaction) with also the operational (velocity, working depth) and environmental (moisture, temperature) conditions. The wear measurement techniques in these investigations were often based on mass loss or dimensional changes. Surface characterization for understanding the wear micro-mechanism has not been done previously. This surface characterization provides information about groove geometry which explicates the particular micro-mechanism based on the D_p value. The wear patterns as such found on the worn tine has been verified with a DEM model.

2. Materials and methods

The tillage tool that is investigated is a symmetrical skew wedge tine, which is globally used for soil cutting and loosening in the first phase of primary tillage. As they are used in the earliest phase of tillage, when the soil has a high compactness, they suffer from severe wear. The tines used in the current investigation were provided by Köckerling. The tine is constructed out of an alloyed martensitic steel 27MnB5. The chemical composition of the tine material of base 450 HV hardness (tested with 100 N load) is shown in Table 1.

The density of 27MnB5 (1.5529) is 7.86 [kg/dm^3], where the tensile strength was measured to be 1575 [MPa] (0.5 mm/s 100 kN on Zwick/Roell Xforce P) and 181 [GPa] Young modulus (determination 10 kN–20 kN). Thirteen independent agricultural tines corresponding to different sliding distance were investigated for the wear trend, specific wear mechanism and also for its material characteristics (microstructure and hardness). The test conditions of the tines are given in Table 2. A total tillage distance was 145 km, which corresponds to 182 ha. Fig. 1 shows the cultivator used with the associated tine positions.

Each tine was field tested for a specific distance as mentioned in the below table. The tines were mounted on a cultivator and the influence of the position difference is assumed to be negligible, tines in the

Table 1
Chemical composition of tine [wt %].

C	Si	Mn	S	P	Cu	Cr
0.285	0.253	1.125	0.001	0.013	0.015	0.165
Ni	Mo	V	Al	Ti	Nb	B
0.011	0.028	0.004	0.041	0.035	0.013	0.003

Table 2
Tine test conditions.

Tine number	0	1	2	3	4	5	6
Distance	0	10.3	21.6	32.8	41.8	53.9	60.7
Soil	–	Loamy sand	Loamy sand	Loamy sand	Loamy sand	Loamy sand	Loamy sand
Mass		1022.40	958.95	939.00	842.90	795.20	777.50
Tine number	7	8	9	10	11	12	13
Distance [km]	73.9	82.9	96.4	109.3	119.9	132.7	145.3
Soil	Loamy sand	Loamy sand	Sandy loam	Sandy loam	Loamy sand	Loamy sand	Loamy sand
Mass [g]	748.65	758.65	744.45	734.00	610.10	591.70	483.85

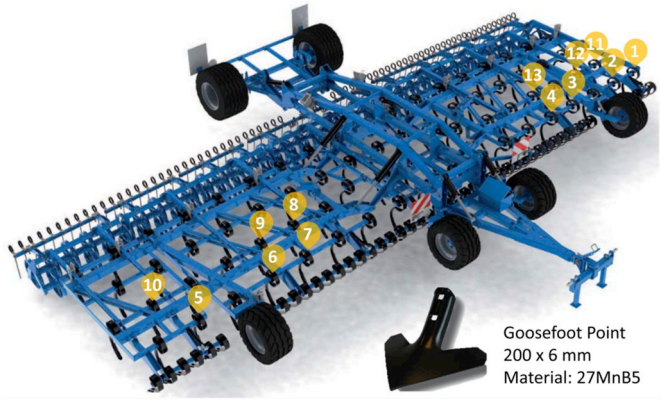

Fig. 1. Tine positions on the cultivator [1].

compacted track of the tractor were not used for this investigation. However, it should be noticed that tines could wear asymmetrically when they were positioned at the outside of the cultivator. This is a consequence of the overlap of the work field during tillage. Working speed during the test was in a range between 8 and 12 km/h and the working depth was between 5 and 8 cm. Two different soil types were involved: loamy sand and sandy loam soil. The tines as received from the field were partially corroded and hence the mass for each of the tines were measured after following a special cleaning procedure.

In the first stage the tines were cleaned with vinegar and LOCTITE SF 7063 to remove the rust and remaining soil particles. Mass loss, linear geometrical and thickness measurements were performed on the cleaned tines with an electronic scale with a resolution of 0.1 g and a caliper with the accuracy of 0.1 mm. To identify the wear micro-mechanism on the tine surfaces, investigation was done using 3D profilometry (Taylor Hobson CCI HD) as well as macrographic information were extracted. Based on this investigation, the regions within the individual tines were segmented geometrically (Fig. 2) to differentiate for the region-specific wear characteristics such as wear mechanism, wear rate, roughness characteristics, microstructure and hardness change.

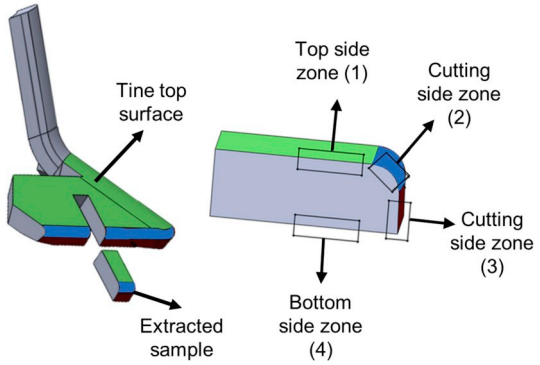

Fig. 2. Geometric segmentation and sample extraction from tine.

The cross-sectional analysis was made on the extracted individual tine samples which covered both previously recognised segments (Fig. 2).

Subsequent polishing and etching allowed to investigate the microstructure (Zeiss AxioCam MRc5) at different magnifications covering the following tine zones: one zone on the top side (green colour), two zones on the cutting side (blue and red colour) and a reference unworn zone (grey colour). Scanning electron microscopy (SEM) investigation was also performed for verification and to acquire more detailed information about the differences in morphology. Hardness measurements were performed using LECO LV 100AT Vickers hardness tester. Furthermore, the surface was studied in detail for its 3D topography using white light interferometry (Taylor Hobson CCI HD) with 10X lens covering 0.8 mm x 0.8 mm area. The cut-off of the measurements was set according to the standard ISO 4287. The surface topography data was extracted from the 3D map to calculate the degree of penetration (D_p). Hokkirigawa et al. [26] introduced a formula that predicts the degree of penetration in a single-asperity contact scratch test for a certain *normal load W* [N] and an *indenter tip radius R* [μm] on a surface with *hardness* [HV]. The equation parameters are

$$D_p = \frac{h}{a} = R\left(\frac{\pi Hv}{2W}\right)^{\frac{1}{2}} - \left(\frac{\pi HvR^2}{2W} - 1\right)^{\frac{1}{2}} \quad (1)$$

The critical value of D_p to set the demarcation between micro-ploughing and micro-cutting is around 0.2 for various attack angle. After a topographic surface characterization measurement it is possible to calculate the mean D_p of all the grooves that are present on the worn surface. Coronado et [27]. validated the following formula for D_p when comparing two abraded surfaces:

$$D_p = \frac{R_z}{\frac{R_{sm}}{2}} \quad (2)$$

where R_z is the ten point height [μm] and R_{sm} [μm] is the mean spacing at mean line. These are corresponding to the groove depth and the groove height of a single scratch. To investigate the abrasive particles the two soil samples from the field test were characterized. Mineralogy results were obtained with X-ray diffraction (Rigaku Ultima IV). Semi-quantitative and mechanical analysis were performed to obtain soil parameters according to MSZ 20135:1999 4.2 and MSZ-08-0206-2: 1978 standards.

The soil flow and tine engagement with the soil particles was further studied to investigate the effect on wear pattern. The particle movement along the goosefoot tine cannot be measured directly. For this reason, this movement is investigated using the DEM. Parameterisation via angle of repose tests, direct shear tests and a comparison of the forces on a reference tool, which were recorded in a soil bin can be assigned soil-like properties to the particles. The particle radius was set to 1 mm and corresponds to be ~5 times larger than the real size of soil particles. The difference in particle size between the simulation and the real soil can be neglected, because the parameters are set via the bulk material properties and not of the individual particles. Fig. 3 shows the goosefoot tine in the DEM simulation with 2 209 000 particles in an 800 mm long particle bed. To reduce the total number of particles, the symmetry axis of the tine is used and only one half moves through the particle bed. The

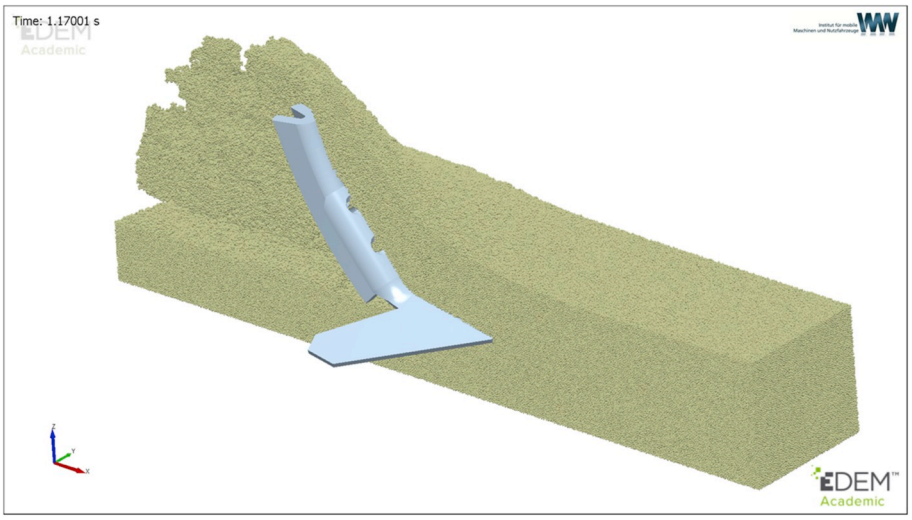

Fig. 3. DEM simulation of a goosefoot tine.

working speed of the tine was 10 km/h with a working depth of 6.5 cm, which corresponds to the average field test values.

3. Results and discussion

3.1. Mass loss and dimension change

Fig. 4 shows all the 13 tines, where the geometrical size reduction due to material removal can be clearly seen. In the present investigation clearly shows the difference between the initial stage and the final stage of wear. A clear reduction over 55% of the mass loss was observed between a new and a fully tested tine. The mass loss of each tine is plotted in function of the operating distance (Fig. 5). A linear trend was observed in the mass loss similar to literature, where the present wear rate of 3.24 g/km from the field investigation is relatively low. The difference compared to the field investigation of Ferguson et al. [7] is due to the aggressive nature of stony soil when compared with the present loamy soil condition. It is clear that the soil type has a significant influence on the wear rate. The result of the soil investigation and the difference in wear rate in the different soils will be discussed in the next paragraph.

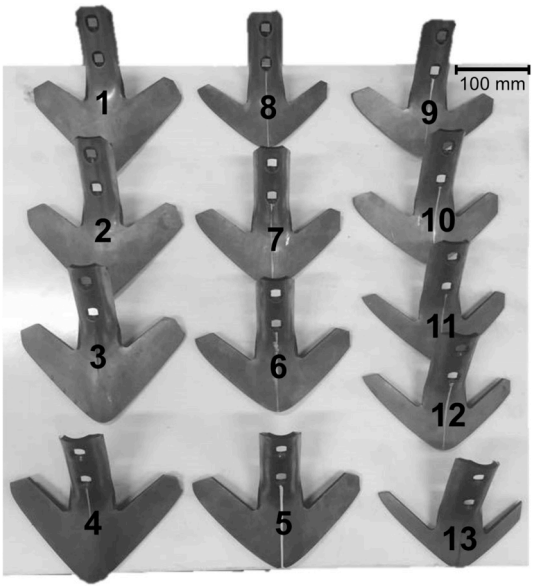

Fig. 4. Wear of tines (1–13) after different sliding conditions.

Apart from the mass loss a change in sharp edge of the tines to a curved geometry is evident. A large decrease in tip and edge length was observed. The shape change in geometry indicates the change in the specific abrasive wear rate in function of operating distance. The reason for this is the change in the operating conditions as well as and the change in the tribo-system because of the different attack angle of the impacting soil particles and the difference in the contact geometry. As the tine is more worn, the projected frontal area/reference area of the tine is decreasing and the contact with the soil particles shifts more to impact of front side rather than sliding with a more sharp angle. Based on these information, further investigation on the effect of the attack angle of the soil in case of tines is to be examined. The defined points for the thickness measurements on the tines, similar to the investigation of Owisak [3], are shown in Fig. 6 a). The result of the thickness measurements is given in Fig. 6 b). The wear is more severe closer to the tine tip, where the stress state is highest together with highest relative velocity.

The thickness can be described as a power function of the working distance. This means that during the first 50 km of usage the tine shape changes the most. Similar results were also found in the investigation by Owsiak [3]. The first 50 km distance was observed as a running-in period of the wear process. Work hardening is expected in this running-in period which then causes a hardened layer that is continuously removed and recreated by the wear process leading to a steady state wear behaviour.

The geometrical dimension loss (tip length, edge length and width) of each tine is shown in Fig. 7. The dimensional measurement points marked with x are outliers and considered as false measurement. The rapid increase in the wear of tip length during the initial period was followed by a linear trend. The material removal is dominant along the cutting edge when compared with the loss of thickness and for this reason priority was given to the surface investigation on the cutting edge.

The present in-field investigation shows similar results to that of [7]. In the initial stage of the wear process the tip length had decreased significantly, but the edge length loss was low. These dimensional changes may be observed as blunting of the tine. After blunting of the tip the tine has a uniform wear rate. The decrease in the width is negligible. When comparing the tip length losses with the thickness reduction it is clear that the wear of the cutting side should be prioritized. The wear of the cutting side caused the largest volume losses of the tine. This confirms the expectations from literature findings introduced earlier, that the wear of the cutting side is more severe than the top surface wear [3,

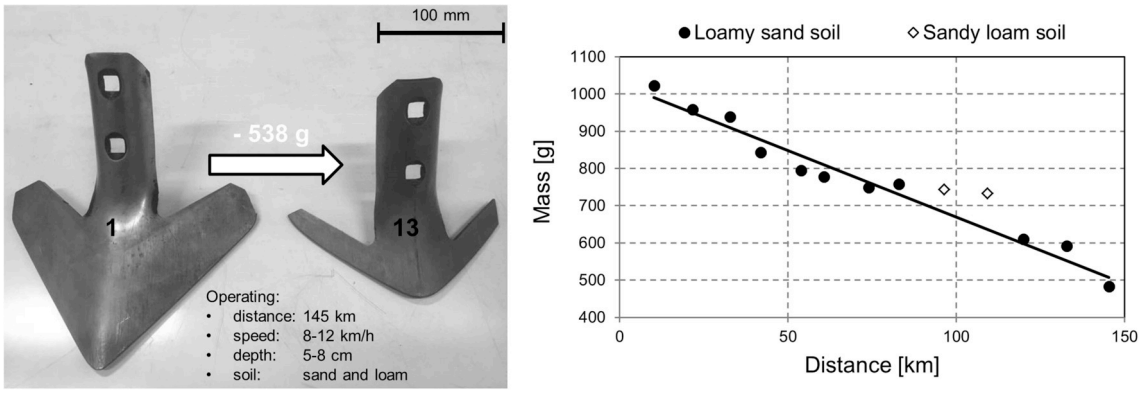

Fig. 5. Mass loss of tines in function of sliding distance.

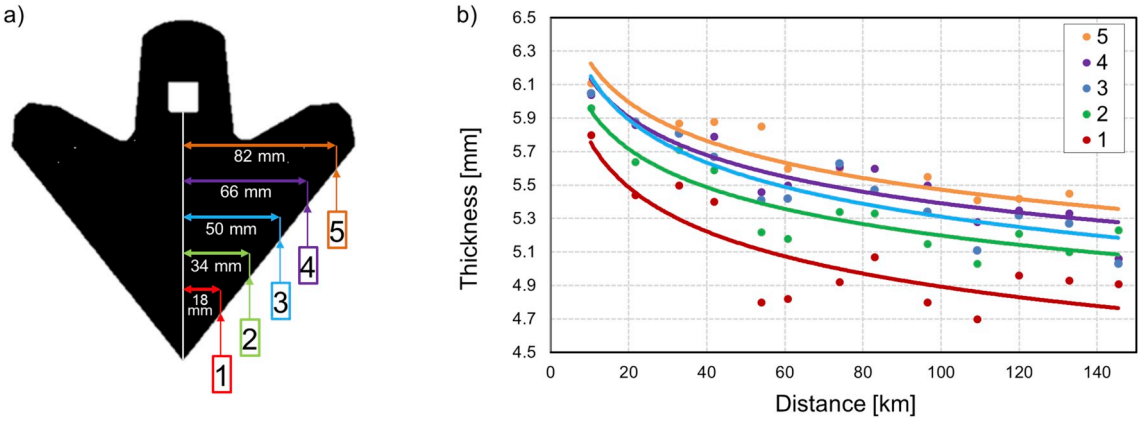

Fig. 6. a) Defined thickness measurement points on the tine b) Result of thickness measurements in function of operating distance of each tine.

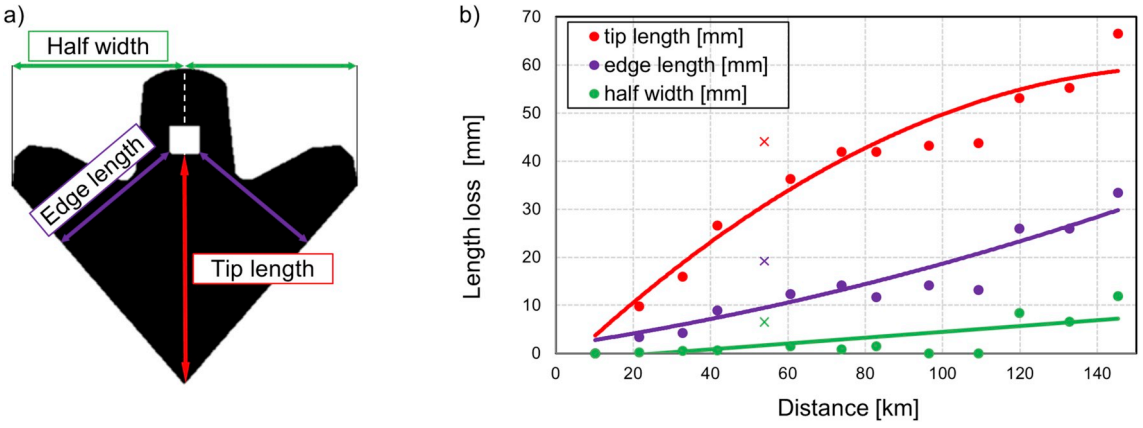

Fig. 7. Geometrical loss of each tine in function of operating distance. a) Tine geometry b) Geometrical loss of each tine in function of operating distance.

8].

The tip shape change was also documented. The wing of the tines were cut in their cross section, where the edge length was measured (Fig. 8 a). The tines were set in a fixed position with their wing cross-section facing a camera. Macro images recorded their geometric boundaries and together with the results from edge length measurements the shape change is investigated. A sketch of the shape change in function of the operating distance is presented in Fig. 8 c) along with the proportional edge length decrease. The shape sketches from tine 1 (10 km), 2 (22 km), 10 (109 km), 13 (145 km) are showing the material loss from the tine top and cutting side as well as the material loss in the edge length. The angle of the tip (α) with respect to the virtual surface perpendicular to the top surface was plotted in Fig. 8 b). The tip angle for an unworn tine is 0. Similar to the thickness loss curves, also a running-in and transition to steady state was observed in the α angle change in function of the operating distance. In the first 20 km the tip angle changed more than in the last 50 km. The angle α described in the figure has a significant influence on the flow of particles along the cutting edge. To enhance wear resistance either the loss in this angle could be prevented or the material must become less sensitive to micro-cutting mechanism.

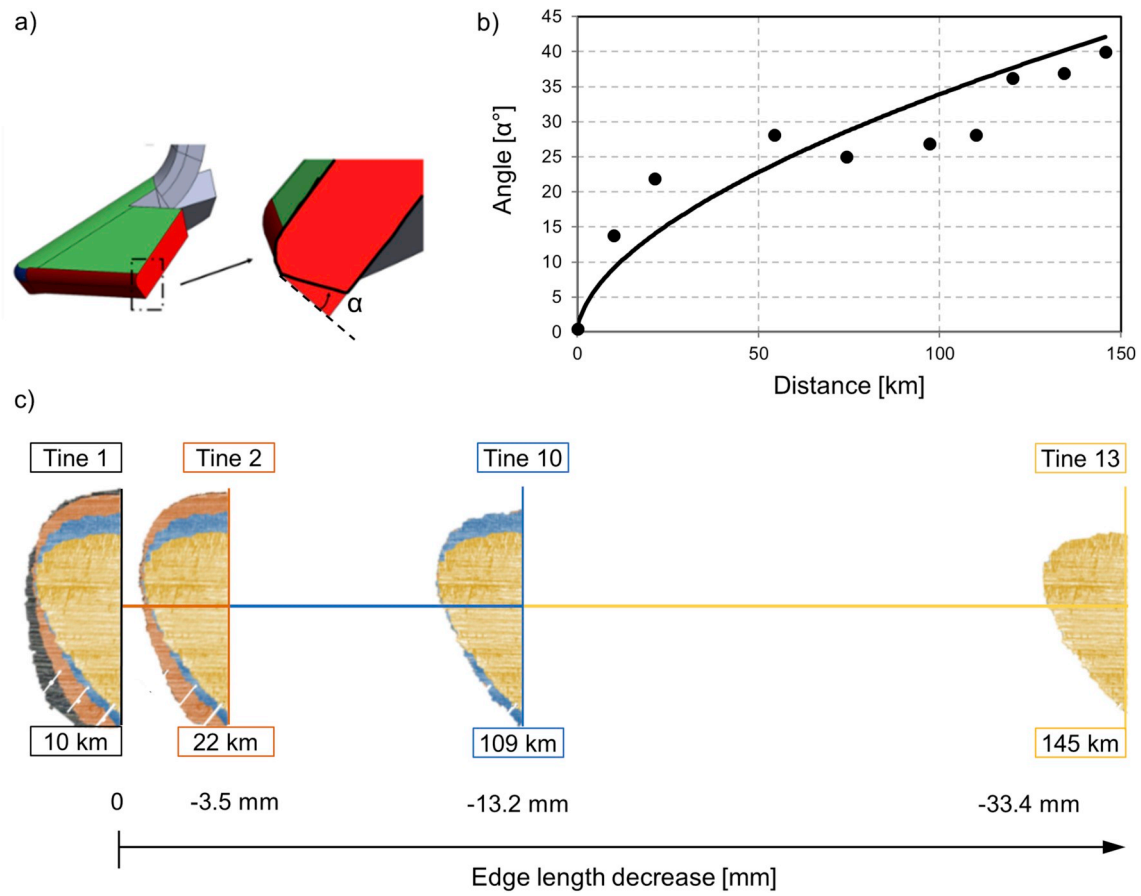

Fig. 8. a) Defined α angle in the tine wing cross section b) Tine α angle change in function of operational distance c) Proportional tine tip shape geometry change with edge length decrease in function of operational distance.

3.2. Soil investigation

The result of the soil analysis showed that the loamy sand and the sandy loam soil are quite similar (Table 3) [28]. The loamy sand soil contains more sand (quartz) fraction and less clay. In the sandy loam a little more humus was measured, which has a positive effect on plants. The average abrasive particle size with the highest distribution was found to be the coarse sand of >0.25 mm [m/m%] and 0.05–0.25 mm [m/m%] fine sand in case of both soil. The average abrasive particle size with the highest distribution may give indication on the wear track width dimension caused by these quartz abrasive particles to be in the range of 20–500 µm. The difference in wear rate in case of the two different soils was confirmed from the mass measurements of the tines. Tines run in the loamy sand experienced an average wear rate of 5.28 g/km, while 0.94 g/km in the sandy loam. The abrasive effect of the ~10 m/m% more sand content of the loamy sand soil may explain this phenomena.

Table 3
Soil characteristics.

Particle content [m/m%]	Soil type	
	Sandy loam	Loamy sand
>0.25 mm coarse sand	35.17	32.06
0.25–0.05 mm fine sand	35.29	47.91
0.05–0.02 mm sandy silt	5.65	6.51
0.02–0.01 mm silt	4.50	4.32
0.01–0.005 mm silt	4.19	1.30
0.005–0.002 mm silty clay	4.45	2.67
<0.002 mm clay	10.75	5.23
fine fraction (<0.02 mm)	23.89	13.52

Compared to other soil types (e.g. loam, clay), high sand percentage soils have a significantly higher abrasive effect on tillage tools, however in these soils no contamination of stones and gravel was found. Other soil parameters such as soil moisture or compaction, but also process parameters such as working depth and speed have a major influence on wear rates according to Owsiak and Ferguson et al. [3,7] and prevent a direct comparison with other publications.

3.3. Surface characteristics

Surface topography and morphological investigation was performed to understand the wear process. The different tine regions were investigated separately.

3.3.1. Top surface

Beside the optical microscopy, white light interferometry was used to understand the transition of surface morphology before and after wear. The results of 3D topography in Fig. 9 clearly shows a random pattern of the painted surface which has been transformed to directional pattern after the wear process. In addition to micro-cutting and micro-ploughing, micro-pitting was also observed. The material removal through pitting could be neglected because only a few micro pits were observed on the worn tine top surface caused by the repetitive alternate loading by impact and sliding. Also, as concluded before the dominant material removal was experienced in the cutting edge of the tines. The orientation of the grooves gives an idea about the tine movement direction.

The tine top region surface topography investigation resulted an average Ra 1–2 µm, Rt 10–15 µm, Rz 7–10 µm, Rsm 90–180 µm across all tines with some wider grooves present as seen in Fig. 10.

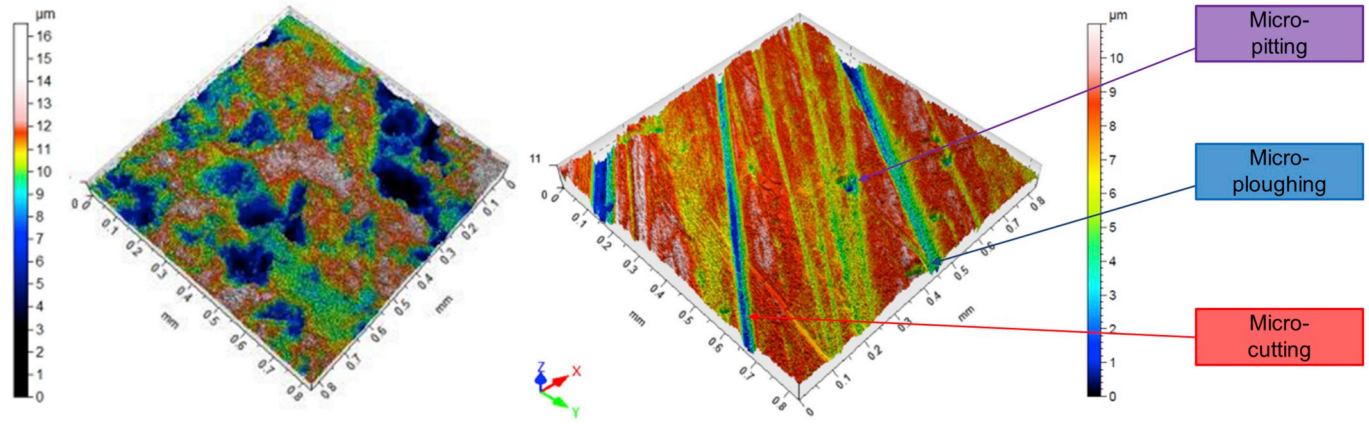

Fig. 9. 3D topography of tine top surface before and after wear (60.7 km operation).

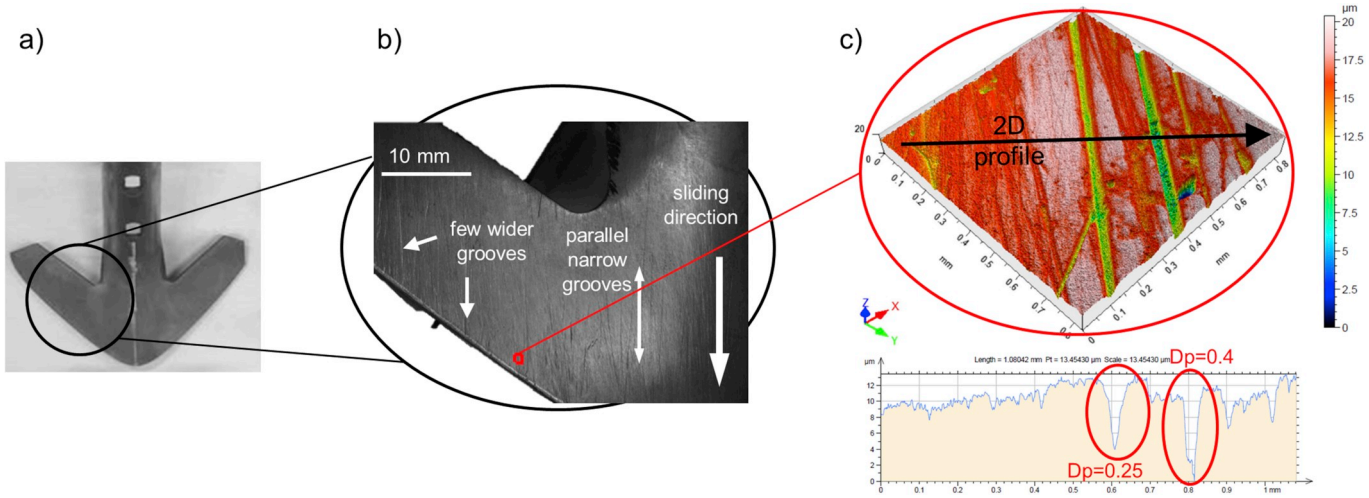

Fig. 10. a) Tine 6 overview b) macro image of tine 6 top surface c) 3D topography of tine 6 top surface and D_p extraction.

Wear micro-mechanisms were characterized with the degree of penetration (D_p) of the abraded groves. The average degree of penetration from the top surface of the tines are in range of 0.31 ± 0.61 [-], and these values indicate micro-cutting mechanism [29]. The visual inspection also showed oriented, narrow parallel grooves which is in line with the D_p values for validating the micro-cutting mechanism, as seen in Fig. 10.

3.3.2. *Cutting side (edge)*

Comparing the thickness reduction to the edge length and tip length,

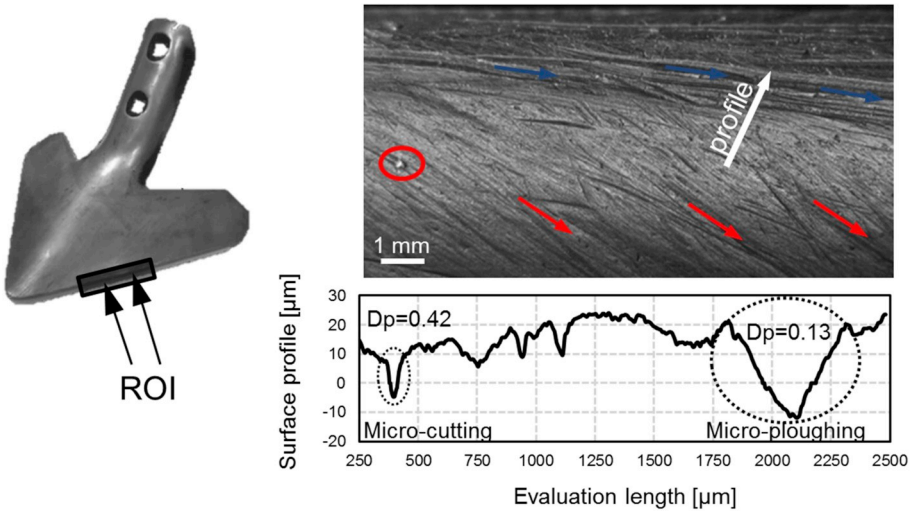

Fig. 11. Macroscopy of tine cutting side surface and D_p extraction.

it is evident that the material removal is dominant along the cutting sides (edges). For this reason, priority was given to the surface investigation on the edges. The arrows in Fig. 11 show the region of interest (ROI) for macroscopy and topography investigation. From the macroscopic investigation two different wear mechanism were observed on the contact surface. The upper region with blue arrows were observed with large, wide grooves with plastically deformed ridges indicating the local plastic deformation (micro-ploughing). The orientation of the grooves is parallel with the sliding direction in this upper part of the cutting side. The bottom region with red arrows experienced micro-cutting mechanism with several small narrow grooves and traces of chip formation. The soil during the initial contact introduces a local plastic deformation which is indicated by the top half area. The direction of the grooves tends to change which may have to do with the flow direction of soil relative to the tine. This allows to conclude that in the compact regions a higher contact pressure may persist and hence micro-cutting is experienced. The surface profilometry and D_p data extraction from the wear grooves confirmed these findings. Macroscopy of the tine cutting side surface and the extracted profile for D_p calculation is shown in Fig. 11.

The lower D_p (compared to the top surface) indicated micro-ploughing and plastically deformed material on the upper part of the cutting edge. The large, wide grooves with plastically deformed ridges, resulted in an average D_p of 0.09 ± 0.05 [-]. D_p range of 0.24 ± 0.05 [-] was measured at the bottom part indicating a dominant micro-cutting phenomena which results into a more uniform wear pattern with narrow parallel grooves [27]. Traces of continuous chip formation marked in red circle (Fig. 11) was also observed in this region verifying the micro-cutting mechanism. The co-existence of these two micro mechanisms observed on the cutting edge with each dominant in a specific region could aid future tine designs aiming at prolonging lifetime. This could be achieved by different heat treatment of the upper and lower zones of the cutting edge. A carefully designed coating on the surface regions which experience more severe wear could be an option too.

Vickers hardness and the microstructural analysis were performed on the cross-section of the sliding interface (Fig. 12). The microscopy covered the following tine zones: one zone on the top side (green colour), two zones on the cutting side (blue and red colour) micro-ploughing and micro-cutting zones, one zone on the bottom (grey colour) side for reference (unworn zone). The microscopic observations showed a tribo-layer on the worn surface. This tribo-layer was present in all regions where the sample was in contact with the soil (top side and cutting side). This thin layer is formed from the hardening, which is a consequence of force interaction between moving surfaces. Due to the local stress concentration, the thickness of the tribo-layer was significant in the micro-ploughing zone, where the thickness of this uniform, plastically deformed layer could reach up to ~50 μm. The pressure results in compression of the plastically deformed material, where the morphological orientation also changes. In this compressed zone a change in the orientation was clearly observed in the microstructure. On the tine top surface, a thin tribo-layer was observed with traces of uneven material shear-off indicated with red arrows in Fig. 12. Thin tribo-layer with similar characteristics of the material boundary was observed on bottom of the tine cutting side. These features may give an indication that micro-cutting mechanism is the dominant phenomena in the material removal in these zones. The unworn bottom tine zone serves as a reference surface without significant changes in its microstructure.

To study the change in morphological orientation and the plastic flow on the contact surface SEM was performed on the extracted tine sample (Fig. 13). From the SEM images the change in morphological orientation was clear, where in the tribo-layer the direction become parallel to the sliding direction (black arrow parallel to the tine zone boundary). In the region where micro-cutting was the dominant micro-mechanism the tribo-layer suffered traces of material shear resulting in uneven surface boundaries (black arrows indicating material shear in top and micro-cutting zones) Due to the repeated material removal from micro-cutting the tribo layer was observed to be few (1–2) μm in thickness. The bottom tine surface was considered as a reference because of the unworn condition. In this area no significant change was observed in the microstructure.

Hardness measurements of these areas (top area, micro-ploughing and micro-cutting zone on the cutting side, bottom area) indicated,

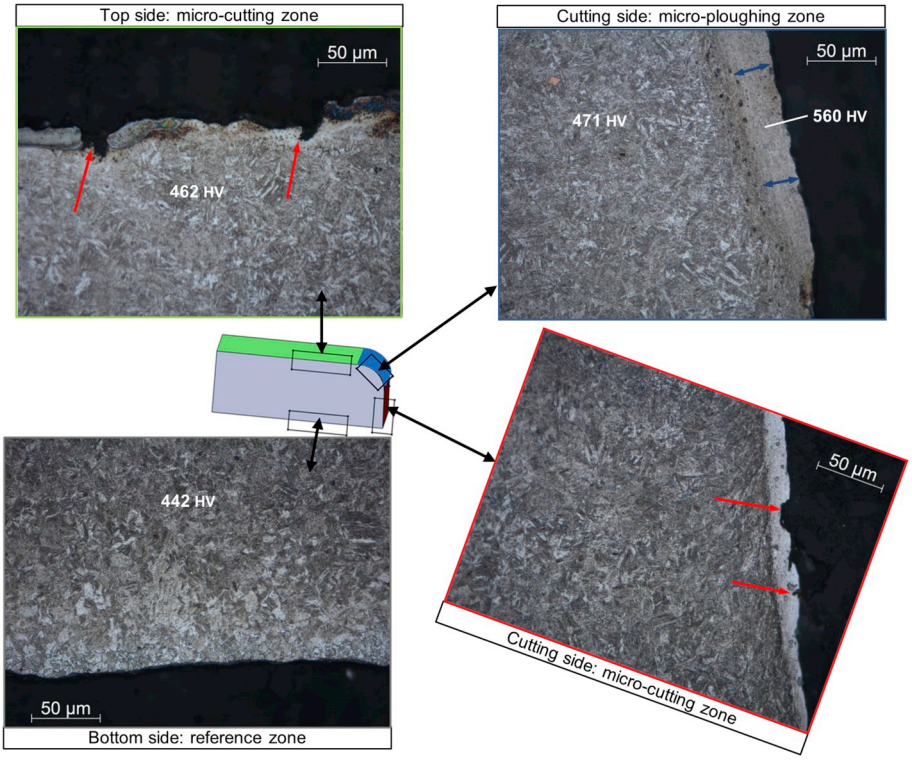

Fig. 12. Optical microscopy of extracted tine sample 12 (132.7 km operation).

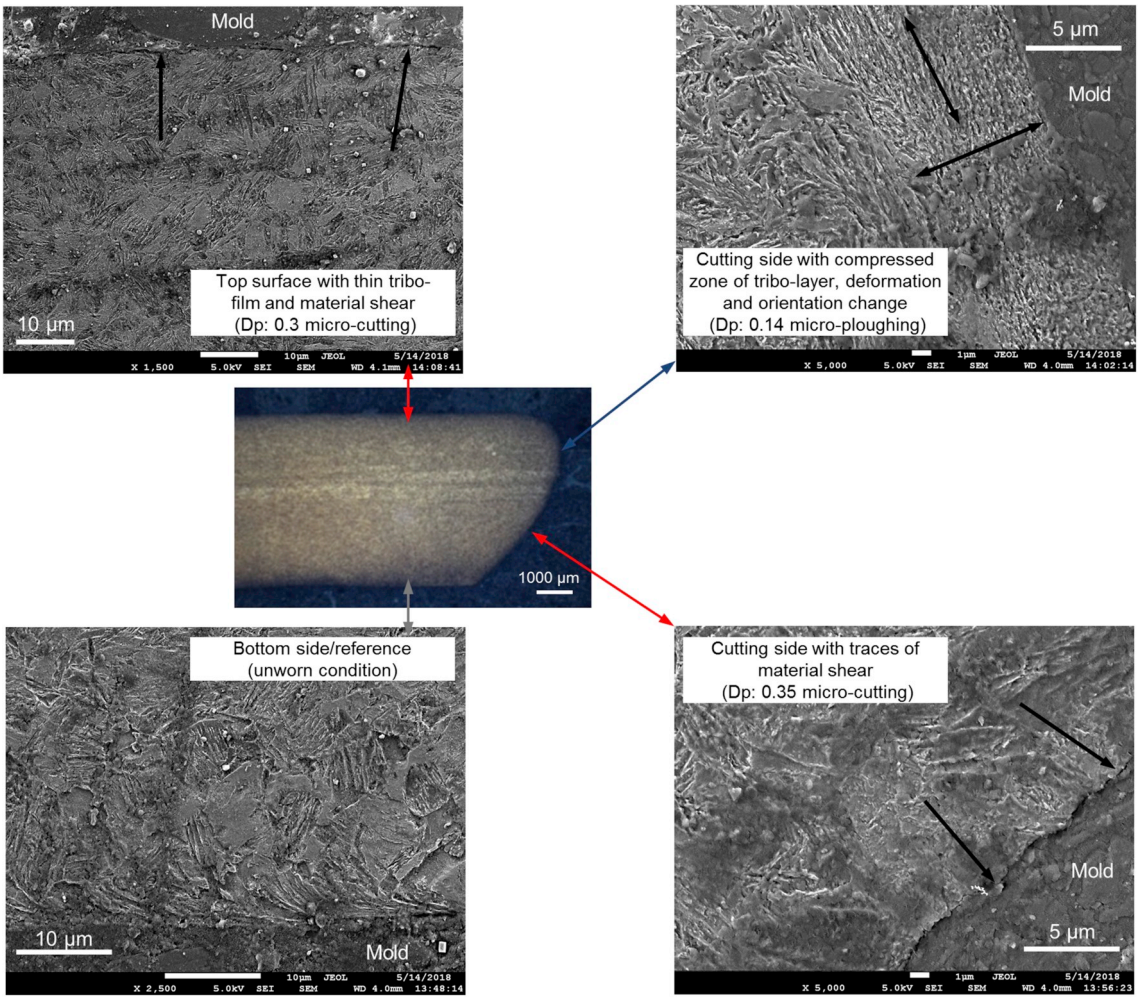

Fig. 13. SEM on extraced tine sample 12 (132.7 km operation).

that the tribo-layer zone has increased hardness with ~110 HV (Table 4). The change in morphological orientation can be observed from the plastic flow of the material in the direction of sliding. As a consequence of compressive stresses grain refinement on the top layer is observed which results in increased hardness. This increase in hardness was already realized after 10 km of sliding distance. The measured hardness of the reference unworn (bottom side) zone remained close to 440 HV.

3.4. Investigation of particle flow with DEM

During the analysis with the DEM, the particle movement along the cutting edge of the tine could be identified more precisely. For this purpose, only individual particles from the particle bed are monitored at one time step (Fig. 14). At this time the submerging phase of the tine into the particle bed is completed and a constant flow has formed. The particles under consideration are initially in contact with the cutting edge of the tine and move away from the tool on its path through the particles. The angle of the cutting edge to the tine top surface (tine wing) is 90°, with the exception of the tip. As a result, the cutting edge is inclined backwards in the mounting position. When looking at the particle movement in the top view (z-axis), as shown in the figure, it can be seen that the particles are covered by the geometry during the tine movement. The tine is shown with reduced opacity.

The particle movement mainly below the cutting edge can also be seen in Fig. 15 in the frontal view.

The path of the particles along the cutting edge is shown in the following Fig. 16. The figure shows the tine in front view (x-axis). The cutting edge is angled in the operating direction so that the front edge of the tine is connected to the upper surface. The movement of the particles until they are submerged: they move perpendicular to the sliding direction of the tines where the particles glide along the cutting edge. Once the particles are submerged, they move parallel towards the sliding direction of the tine against the cutting edge. The particles move sideways along the cutting edge to the outside as can be seen by their track. The scratches on the macroscopic images is also shown.

Similarities can be seen in the comparison of the simulation results with the macroscopic image of the cutting edge. In the upper area of the cutting edge there is also a lateral movement of the particles relative to the cutting edge, which becomes steeper when leaving the upper third of the cutting edge. Tracing the movement of the soil particles gives an

Table 4
Zone specific hardness [HV] change of tines.

Tine number	Run [km]	Tine region	Hardness [HV]	Deviation
Tine 1	10	Top side (tine wing surface)	464.7	7
Tine 1	10	Bottom side (unworn reference)	442.4	9
Tine 12	124	Top side (tine wing surface)	473.2	12
Tine 12	124	Bottom side (unworn reference)	438.5	7

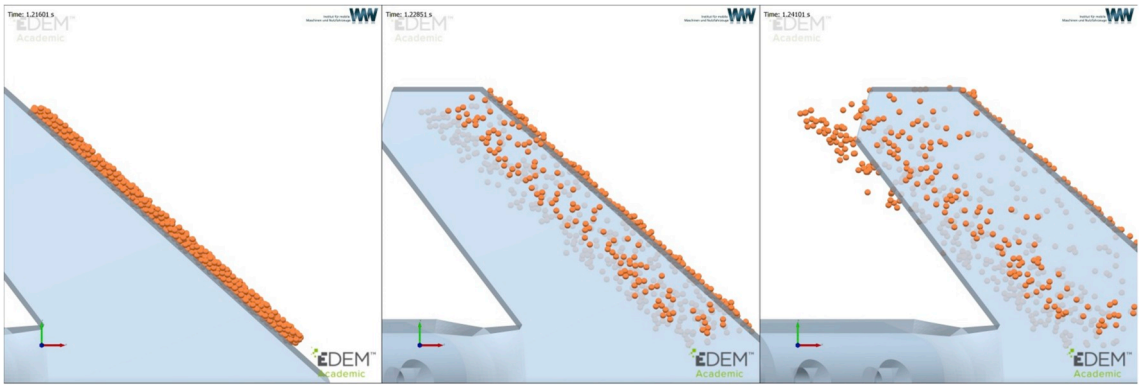

Fig. 14. Soil particle movement along the cutting edge in the DEM analysis.

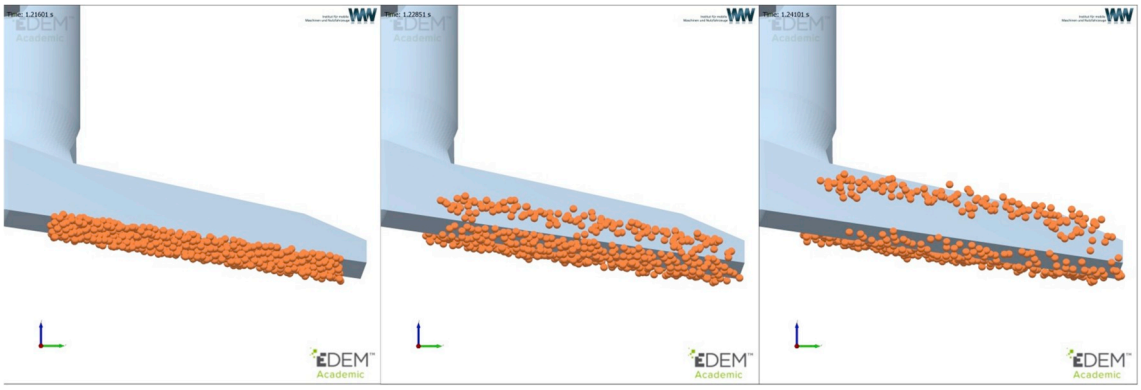

Fig. 15. Frontal view of the particle movement along the cutting edge.

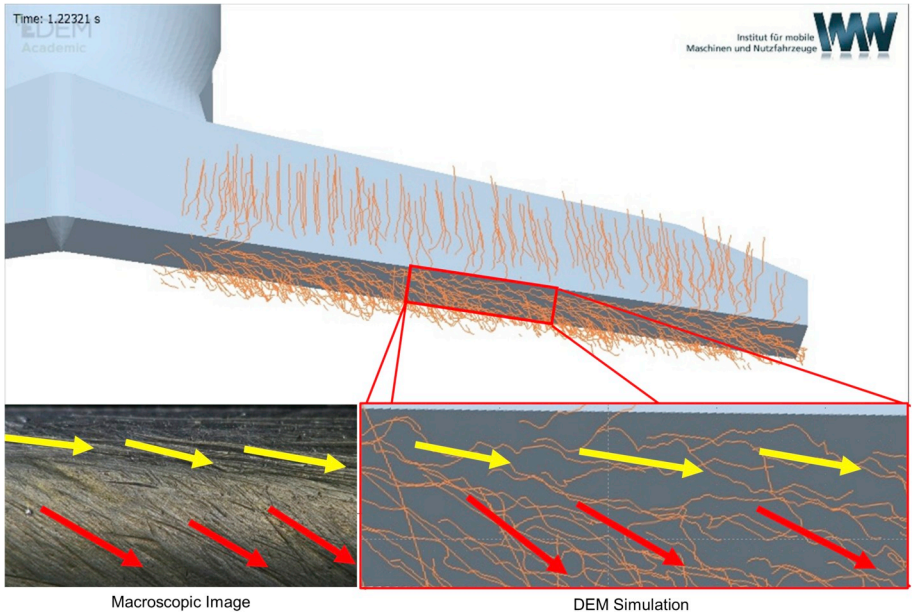

Fig. 16. Path of soil particles along the cutting edge compared with the scratches observed on the surface.

indication on the experienced wear pattern of the tine.

4. Conclusions

Based on the mass loss measurements and change in geometrical dimensions the wear trends obtained from the in-field test are in good agreement with literature of symmetrical goose foot tines. Rapid increase in the wear of tip length during the initial period was followed by a linearly increasing trend. A linear decrease in the absolute mass was observed during the wear process, however this is well reflected in the reduction of the tip and edge length rather than the thickness. The material removal was concluded to be dominant along the tine cutting

edges. As the outcome of the in-field testing, sector specific wear mechanisms were identified in different regions of an individual tine. Two dominant micro-mechanisms micro-cutting and micro-ploughing were observed. Material is removed during micro-cutting, with possible wedge formation, however, micro-ploughing results material flow and plastic deformation with built-up ridges without material removal. The tine geometry was segmented based on the observed micro-mechanisms:

(1) Top area (tine wing surface) resulted average D_p for the grooves in the range of 0.46 ± 0.15 [-], these values indicate micro-cutting regime.
(2) The upper part of the cutting edge was characterized by large, wide grooves with plastically deformed ridges with D_p value 0.09 ± 0.05 [-], which is in the micro-ploughing regime
(3) The lower half of the cutting edge showed similar characteristics with the top area with D_p in the range of 0.24 ± 0.05 [-]

DEM simulation of the soil flow in contact with the tine confirmed the observed wear patterns and directions. It was found that on the upper part of the cutting edge the particles move along the edge after the initial contact resulting a plastic deformation of the material. The bottom region which wears off with the described tine tip angle (α) experienced micro-cutting and gliding of the soil particles in parallel with the sliding direction against the cutting edge.

Future design of tine materials could be focused to enhance the wear resistance against micro-cutting, which could prolong lifetime of the tines and hence reduce economic losses. A further possibility to improve the wear resistance is to change the tine geometry. The effects of change in cutting edge geometry can be investigated using the DEM model and evaluated with regard to the wear potential using the relative movement and the load on the tine.

Acknowledgements

The authors would like to acknowledge to Köckerling for providing the tine material and to dr. Haithem Ben Hamouda for the SEM investigation. The authors are grateful to ir. Fabien Taillieu and dr. Wouter Ost for their support on experimental activities and to dr. Barczi Attila for the soil analysis carried out at Szent István University. This work was supported by Research Fund for Coal and Steel (RFCS) project RFSR-CT-2015-00010.

References

[1] https://www.koeckerling.de/products/tillage/cultivator/allrounder-classic/?L=1 (2019.02.17). (Accessed 17 February 2019).
[2] E. McKyes, Soil Cutting and Tillage, Elsevier, 1985.
[3] Z. Owsiak, Wear of symmetrical wedge-shaped tillage tools, Soil Tillage Res. 43 (1997) 295–308, https://doi.org/10.1016/S0167-1987(97)00020-2.
[4] G. Kalacska, Laboratory modelling of abrasive wear effects of soils, Cereal Res. Commun. 36 (2008) 907–910.
[5] National Research Council Canada, F. and L. Associate Committee on Tribology, (Wear, A Strategy for Tribology in Canada: Enhancing Reliability and Efficiency through the Reduction of Wear and Friction, NRC, Ottawa, 1986.
[6] R.W. Fitzpatrick, T.W. Riley, M.J. Wright, J.M. Fielke, P.J. Butterworth, B. G. Richards, P. Peter, J. McThompson, M.G. Slattery, D. Chin, S.G. McClure, J. S. Lundy, End of Grant Report (1988-1990), Australian Wheat Research council, 1990.
[7] S.A. Ferguson, J.M. Fielke, T.W. Riley, Wear of cultivator shares in abrasive south Australian soils, J. Agric. Eng. Res. 69 (1998) 99–105, https://doi.org/10.1006/jaer.1997.0182.
[8] A. Natsis, G. Petropoulos, C. Pandazaras, Influence of local soil conditions on mouldboard ploughshare abrasive wear, Tribol. Int. 41 (2008) 151–157, https://doi.org/10.1016/j.triboint.2007.06.002.
[9] J.M. Fielke, T.W. Riley, M.G. Slattery, R.W. Fitzpatrick, Comparison of tillage forces and wear rates of pressed and cast cultivator shares, Soil Tillage Res. 25 (1993) 317–328, https://doi.org/10.1016/0167-1987(93)90030-S.
[10] J.M. Fielke, Interactions of the cutting edge of tillage implements with soil, J. Agric. Eng. Res. 63 (1996) 61–71, https://doi.org/10.1006/jaer.1996.0008.
[11] H.-J. Yu, S.D. Bhole, Development of a prototype abrasive wear tester for tillage tool materials, Tribol. Int. 23 (1990) 309–316, https://doi.org/10.1016/0301-679X(90)90004-9.
[12] A. Misra, I. Finnie, A classification of three-body abrasive wear and design of a new tester, Wear 60 (1980) 111–121, https://doi.org/10.1016/0043-1648(80)90252-5.
[13] E. Rabinowicz, L.A. Dunn, P.G. Russell, A study of abrasive wear under three-body conditions, Wear 4 (1961) 345–355, https://doi.org/10.1016/0043-1648(61)90002-3.
[14] P.A. Swanson, Comparison of laboratory abrasion tests and field tests of materials used in tillage equipment, Tribol. Wear Test Sel. Des. Appl. (1993), https://doi.org/10.1520/STP15966S.
[15] R.G. Bayer, Mechanical Wear Fundamentals and Testing, second ed., M. Dekker, New York, 2004.
[16] R.G. Bayer, Wear Analysis for Engineers, HNB, New York (N.Y.), 2002.
[17] K. Hokkirigawa, K. Kato, Z.Z. Li, The effect of hardness on the transition of the abrasive wear mechanism of steels, Wear 123 (1988) 241–251, https://doi.org/10.1016/0043-1648(88)90102-0.
[18] P.A. Cundall, O.D.L. Strack, A discrete numerical model for granular assemblies, Geotechnique 29 (1979) 47–65, https://doi.org/10.1680/geot.1979.29.1.47.
[19] C.J. Coetzee, D.N.J. Els, Calibration of granular material parameters for DEM modelling and numerical verification by blade–granular material interaction, J. Terramechanics 46 (2009) 15–26, https://doi.org/10.1016/j.jterra.2008.12.004.
[20] J. Barr, M. Ucqul, J.M.A. Desbiolles, J.M. Fielke, Simulating the effect of rake angle on narrow opener performance with the discrete element method, Biosyst. Eng. 171 (2018) 1–15, https://doi.org/10.1016/j.biosystemseng.2018.04.013.
[21] I. Shmulevich, Z. Asaf, D. Rubinstein, Interaction between soil and a wide cutting blade using the discrete element method, Soil Tillage Res. 97 (2007) 37–50, https://doi.org/10.1016/j.still.2007.08.009.
[22] C. Hang, X. Gao, M. Yuan, Y. Huang, R. Zhu, Discrete element simulations and experiments of soil disturbance as affected by the tine spacing of subsoiler, Biosyst. Eng. 168 (2017) 73–82, https://doi.org/10.1016/j.biosystemseng.2017.03.008.
[23] R. Zhang, B. Chen, J. Li, S. Xu, DEM simulation of clod crushing by bionic bulldozing plate, J. Bionics Eng. 5 (2008) 72–78, https://doi.org/10.1016/S1672-6529(08)60075-X.
[24] L. Graff, M. Roberge, T. Crowe, Application of discrete element method (DEM) simulations as a tool for predicting tillage tool wear, Can. Soc. Bioeng. (n.d.) 1–10.
[25] J. Tong, M.A. Mohammad, J. Zhang, Y. Ma, B. Rong, D. Chen, C. Menon, DEM numerical simulation of abrasive wear characteristics of a bioinspired ridged surface, J. Bionics Eng. 7 (2010) 175–181, https://doi.org/10.1016/S1672-6529(09)60206-7.
[26] K. Hokkirigawa, K. Kato, An experimental and theoretical investigation of ploughing, cutting and wedge formation during abrasive wear, Tribol. Int. 21 (1988) 51–57, https://doi.org/10.1016/0301-679X(88)90128-4.
[27] J.J. Coronado, A. Sinatora, Effect of abrasive size on wear of metallic materials and its relationship with microchips morphology and wear micromechanisms: Part 1, Wear 271 (2011) 1794–1803, https://doi.org/10.1016/j.wear.2011.01.078.
[28] Relation of constituents of fine earth by size, defining textural classes and sand subclasses, in: Guidel. Soil Descr., fourth ed., Food and agriculture organization of the united nations, Rome, 2006, p. 27.
[29] T. Kayaba, K. Hokkirigawa, K. Kato, Analysis of the abrasive wear mechanism by successive observations of wear processes in a scanning electron microscope, Wear 110 (1986) 419–430.